Electronic Supplementary Material (ESI) for RSC Advances.

Supporting Information

Sulfur-doped porous carbon nanosheets as high performance electrocatalysts in PhotoFuelCells

Stavroula Sfaelou[a], *Xiaodong Zhuang*[b], *Xinliang Feng*[b,c]*, *Panagiotis Lianos*[a]*,

[a] Department of Chemical Engineering, University of Patras, 26500 Patras, Greece

[b] School of Chemistry and Chemical Engineering, Shanghai Jiao Tong University, 200240 Shanghai, China

[c] Center for Advancing Electronics Dresden (cfaed) & Department of Chemistry and Food Chemistry, Technische Universitaet Dresden, 01062 Dresden, Germany

Additional diagrams

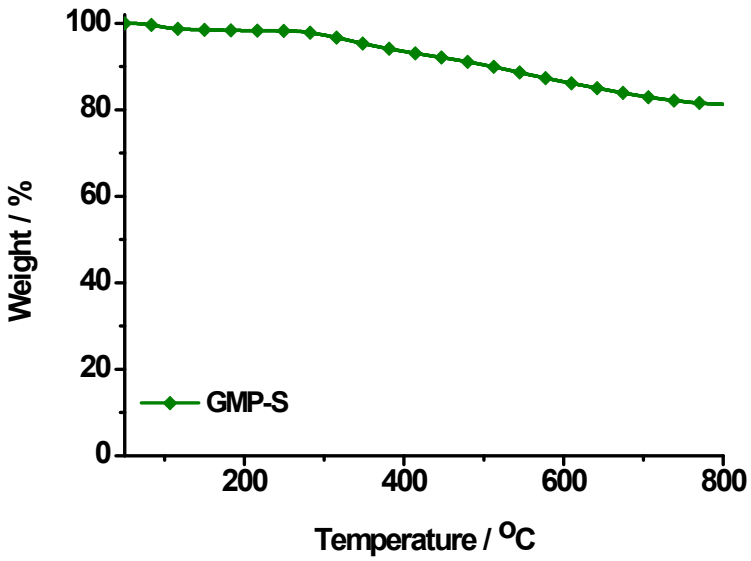

Figure S1. TGA curve of GMP-S.

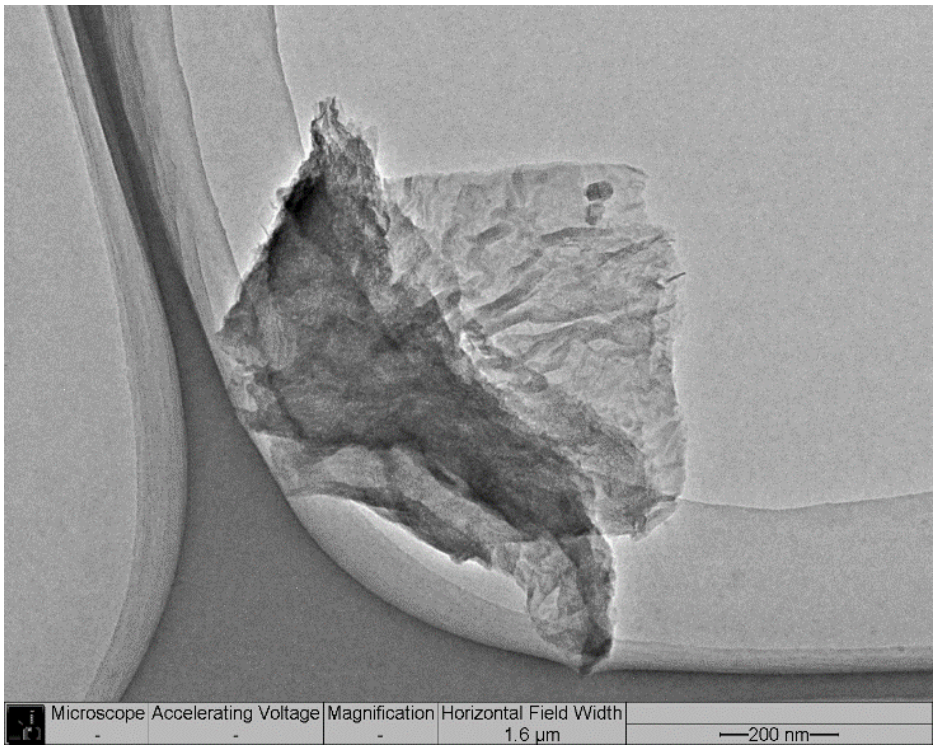

Figure S2. TEM image of GMC-S900.

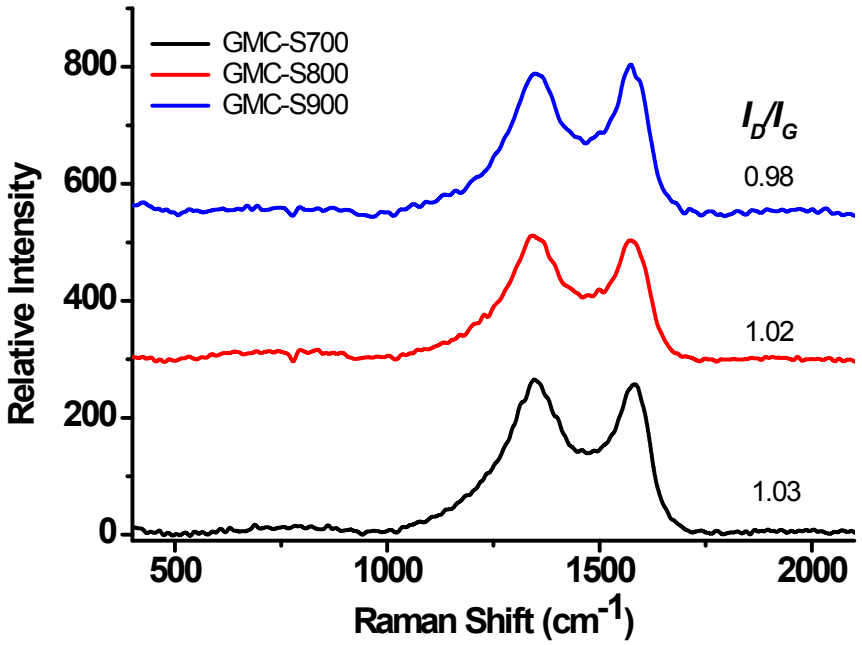

Figure S3. Raman spectra for GMC-S700, GMC-S800, GMC-S900.

Raman spectroscopy is used to elucidate vibrational, rotational, and other low-frequency modes in a system, and has been widely used to characterize the structure of carbon materials, particularly the defects and the degree of ordering of carbon. **Figure S3** shows the Raman spectra of GMC-S. There are two prominent peaks at 1348 and 1579 cm-1, corresponding to the D and G bands, respectively. As is known, the G band is related to the E2g vibration mode of sp2 carbon domains, which can be used to explain the degree of graphitization, while the D band is associated with structural defects and partially disordered structures of sp2 domains. The ID/IG ratio of GMC-S (0.98–1.03) indicates more defects and disordering under high temperature treatment, which implies that partial sp2 domains are restored at different levels, and the graphitic degree for carbonized samples is improved at these temperatures.

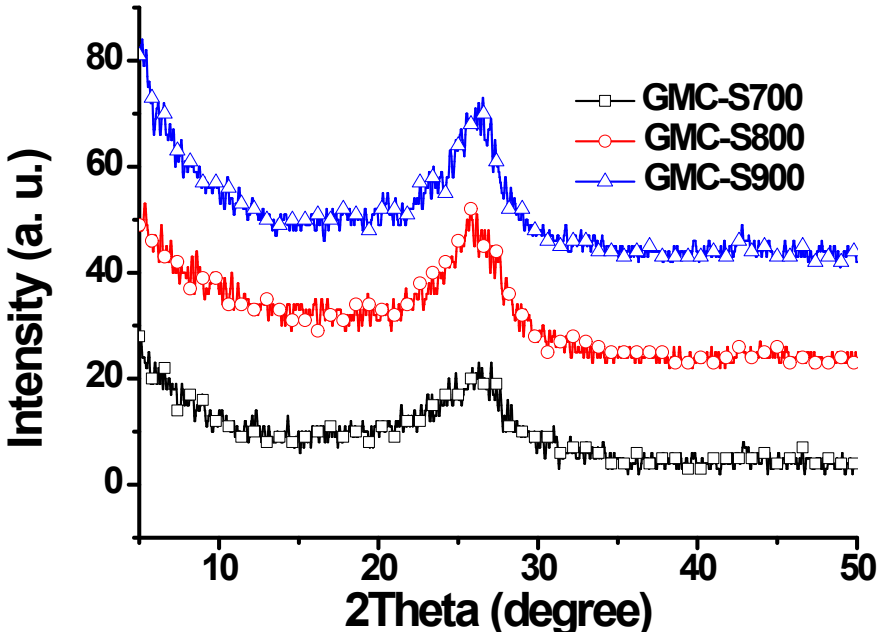

Figure S4. XRD spectra for GMC-S700, GMC-S800, GMC-S900.

The XRD patterns of GMC-S are shown in **Figure S4**. Thermal treatment causes the decomposition of polymer networks and results in new carbon materials with partial crystalline structure. GMC-S700, GMC-S800 and GMC-S900 all exhibit broad diffraction peaks at around 26.2°, which correspond to the plane (002) of graphitic carbon with an interlayer spacing of 0.340 nm. The peak intensities of GMC-Ss increase upon elevating the pyrolysis temperature, suggesting enhanced graphitization on high-temperature treatment.

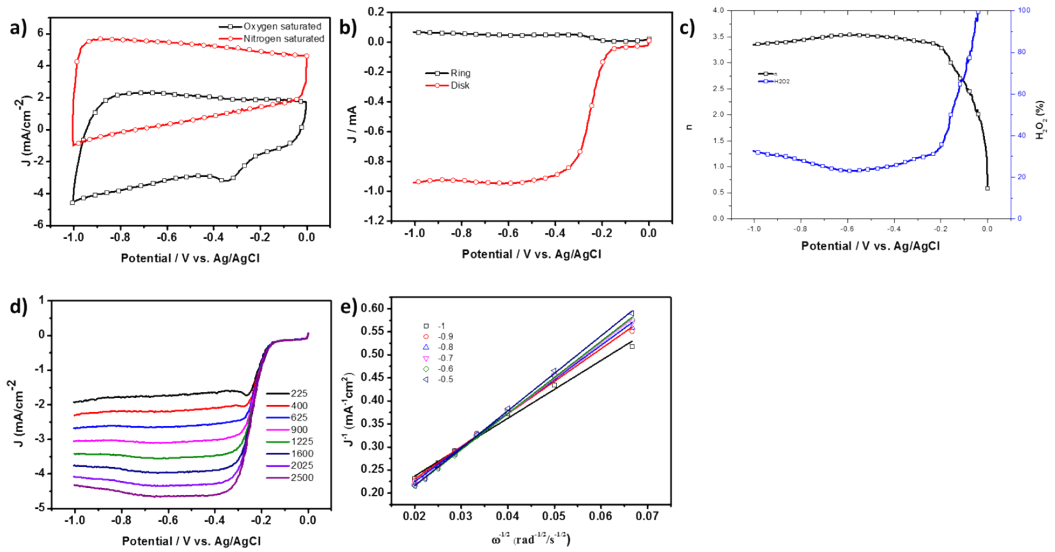

Figure S5. (a) CV curves of GMC-S700 in N2-saturated and O_2-saturated 0.5 M NaOH at a scan rate of 50 mV s^{-1}; (b) RRDE curve of GMC-S700 at 1600 rpm; (c) Calculated electron transfer number and percentage of peroxide; (d) RDE curves of GMC-S700 in O_2-saturated 0.5 M NaOH with different speeds (225-2500 rpm) at a scan rate of 5 mV s^{-1}; (e) Koutecky–Levich plots of GMC-S700 derived from RDE voltammograms at different electrode potentials.

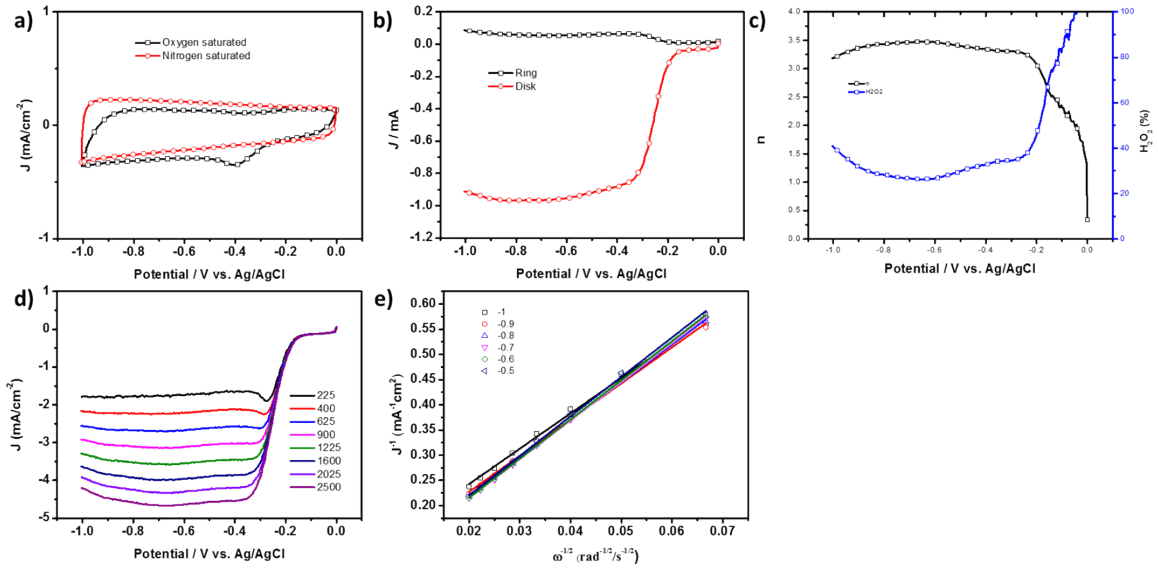

Figure S6. (a) CV curves of GMC-S800 in N2-saturated and O_2-saturated 0.5 M NaOH at a scan rate of 50 mV s^{-1}; (b) RRDE curve of GMC-S800 at 1600 rpm; (c) Calculated electron transfer number and percentage of peroxide; (d) RDE curves of GMC-S700 in O_2-saturated 0.5 M NaOH with different speeds (225-2500 rpm) at a scan rate of 5 mV s^{-1}; (e) Koutecky–Levich plots of GMC-S800 derived from RDE voltammograms at different electrode potentials.

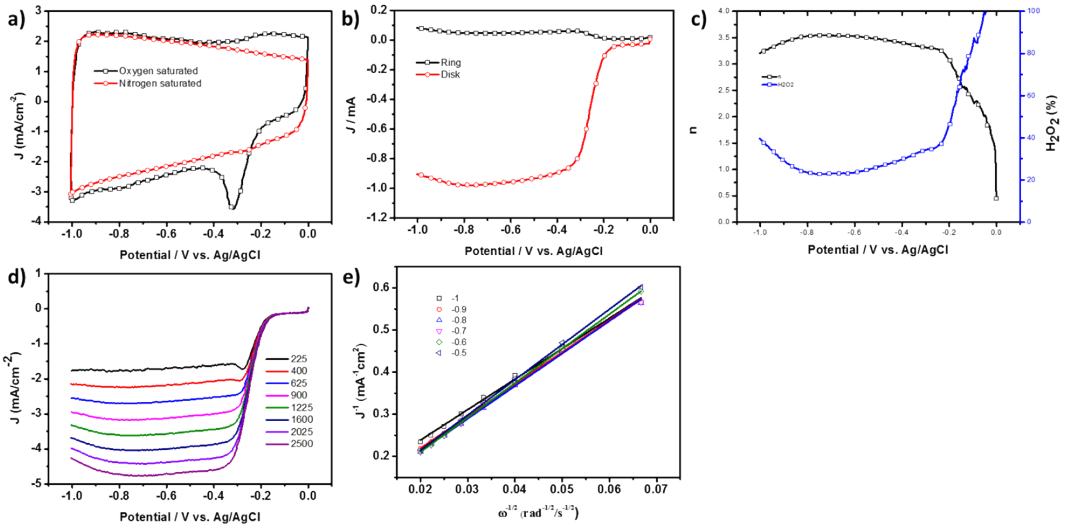

Figure S7. (a) CV curves of GMC-S900 in N_2-saturated and O_2-saturated 0.5 M NaOH at a scan rate of 50 mV s^{-1}; (b) RRDE curve of GMC-S900 at 1600 rpm; (c) Calculated electron transfer number and percentage of peroxide; (d) RDE curves of GMC-S700 in O_2-saturated 0.5 M NaOH with different speeds (225-2500 rpm) at a scan rate of 5 mV s^{-1}; (e) Koutecky–Levich plots of GMC-S900 derived from RDE voltammograms at different electrode potentials.

Table S1. J_k values calculated from K-L plots at different potentials vs. Ag/AgCl for GMC-S700/800/900

Potential	GMC-S700	GMC-S800	GMC-S900
-1.0 V	8.95	9.74	10.62
-0.9 V	11.21	11.89	14.79
-0.8 V	12.93	14.30	16.99
-0.7 V	15.72	16.37	17.36
-0.6 V	16.82	16.65	21.36
-0.5 V	18.57	15.61	21.08